Drug Delivery

DOI: 10.1002/ange.201302557

A Controlled-Release Nanocarrier with Extracellular pH Value Driven Tumor Targeting and Translocation for Drug Delivery**

Zilong Zhao, Hongmin Meng, Nannan Wang, Michael J. Donovan, Ting Fu, Mingxu You, Zhuo Chen, Xiaobing Zhang, and Weihong Tan**

Over the past decades, nanoparticle-based drug-delivery systems (DDS) have received extensive attention in cancer therapy owing to their improved pharmacokinetics and pharmacodynamics arising from the enhanced permeation and retention (EPR) effect.[1,2] To date, many passive targeting systems based on EPR, such as polymeric nanoparticles,[3] liposomes,[4] and mesoporous silica nanoparticles (MSNs),[5] have been constructed to deliver drugs and improve their therapeutic effect. Although the passive targeting approaches can enhance the accumulation of drug in tumor tissue, they do have several limitations.[2] In particular, the random diffusion of drugs in tumor tissue makes it difficult to control the process, possibly inducing multiple-drug resistance. In addition, the EPR effect is small, or non-existent, in certain tumors.[6] To overcome these limitations, biomarker-targeting ligands, such as antibodies, aptamers, and peptides, have been used to further improve the passive targeting systems and concentrate drugs in cancer cells by actively targeting cancer cells after extravasation.[1,7] However, many tumor biomarkers are expressed in both cancer cells and healthy cells, leading to side effects in patients.[8] Further, the strategy based on targeting a specific binding site is impeded by the heterogeneity of tumors, especially the differences among cells within a tumor.[9] Therefore, it is important to explore a general feature of cancer physiology that will allow nanoparticle targeting DDS, without relying on passive retention or on endogenous biomarkers.

The challenges can be addressed by tumor microenvironment-targeting DDS. Acidosis is a typical characteristic of solid tumor microenvironments, and most human tumors exhibit pH values between 6.15 and 7.40 (the latter value representing the mean pH value of arterial blood) that may serve as a general tumor biomarker.[10] Compared with the targeting of molecular biomarkers, the targeting of tumor extracellular pH value (pH_e) is insensitive to protein heterogeneity and is also not limited by the numbers of biomarkers on the cell surface.[11] Thus, various pH_e-triggered drug delivery systems have been designed to improve therapeutic effect.[12] Typical examples are polymeric nanoparticle systems that change their physical and chemical properties, such as their charges[12c,d] or TAT peptide exposure,[12e–g] in response to cleavage of pH-labile groups under the stimulus of local pH_e. All these strategies elegantly surmount the dependence on biomarker and passive retention. However, such technology requires highly sophisticated design to respond to the pH_e stimulus. In addition, the preparation of these polymeric nanoparticle systems is time-consuming and requires a technical knowledge of synthesis.

Recently, a 38-aa peptide named as pH (low) insertion peptide (pHLIP) has been demonstrated to actively and rapidly insert into the lipid bilayer and translocate its C-terminal tail into cells. This occurs by formation of a rigid helix upon change of the pH value from 7.4 to 6.5,[13] providing a novel platform for development of DDS. Herein, we report the use of this peptide to construct pH_e-targeting and intracellular controlled-release nanoparticle-based DDS for drug delivery and tumor therapy (Scheme 1). Based on its highly homogeneous porosity, inertness, biocompatibility, high payload capacity, and easy surface functionalization,[14] MSN, in particular, MCM-41, was chosen as an inorganic scaffold to load anticancer drug doxorubicin (Dox). A pH_e-driven targeting and translocating nanocarrier is achieved by attaching pHLIPss, which is constructed by conjugating a side peptide chain to pHLIP by a disulfide bond at a cysteine residue in the C-terminus (Supporting Information and Table S1), to the surface of MCM-41. In this system, pHLIPss will serve two roles: pH_e-targeting probe and MSN gatekeeper. At pH 7.4, the pHLIPss-MSN nanocarrier is loosely associated with the cellular membrane. Once exposed to pH_e, pHLIPss will rapidly insert into membrane and then translocate MSNs into cells cytoplasm, where the disulfide bonds in pHLIPss will be cleaved and pHLIP will leave from the surface of MSNs, leading to drug release and cell death, due to the presence of reduced glutathione (GSH).

Mesoporous silica MCM-41 nanoparticles were synthesized by a base-catalyzed sol–gel procedure.[15] Transmission electron microscopy (TEM) images and dynamic light scattering (DLS) measurements showed that the as-synthesized MSNs were almost monodisperse nanoparticles with a narrow diameter distribution centered at 140 nm (Figure 1c,d) and pore size distribution centered at 3 nm (Supporting Information, Figure S1a, S1c). Their surface was first

[*] Dr. Z. Zhao, H. Meng, N. Wang, M. J. Donovan, T. Fu, Dr. M. You, Prof. Z. Chen, Prof. X. Zhang, Prof. W. Tan
Molecular Science and Biomedicine Laboratory, State Key Laboratory of Chemo/Biosensing and Chemometrics, College of Biology and College of Chemistry and Chemical Engineering, Collaborative Innovation Center for Chemistry and, Molecular Medicine Hunan University
Changsha, 410082 (China)
E-mail: xbzhang@hnu.edu.cn
tan@chem.ufl.edu

[**] This work is supported by the National Key Scientific Program of China (2011CB911000), the Foundation for Innovative Research Groups of NSFC (Grant 21221003), and China National Instrumentation Program 2011YQ03012412.

Supporting information for this article is available on the WWW under http://dx.doi.org/10.1002/anie.201302557.

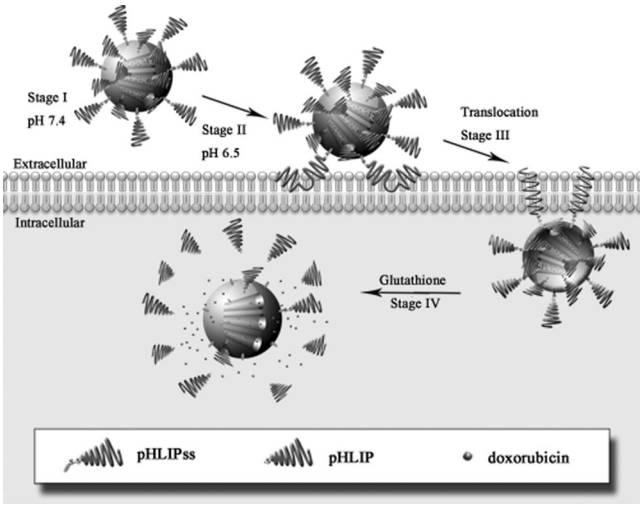

Scheme 1. Targeting and translocation of a pHLIPss-MSN nanocarrier driven by low pH value and the cytoplasmic drug release from the pHLIPss-MSN nanocarrier through disulfide bond cleavage. Stage I: At physiological pH 7.4, the pHLIPss-MSN nanocarrier is loosely associated with the cellular membrane. Stage II: Upon exposure to pH 6.5, pHLIPss spontaneously form helical structures and insert into the lipid membrane. Stage III: pHLIPss-MSN nanocarriers are swiftly translocated into the cell at pH 6.5. Stage IV: The cargo is released by disulfide bond cleavage and the pHLIP leave.

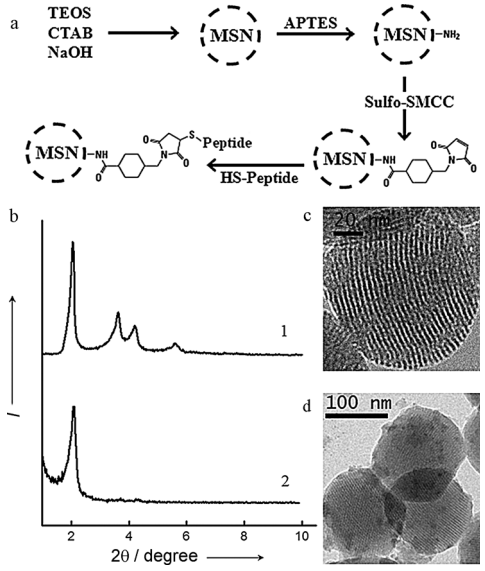

Figure 1. a) Strategies for MSN functionalized with peptide containing cysteine residue by using sulfo-SMCC. b) Small-angle XRD of MSNs (1) and Dox-loaded pHLIPss-MSNs (2); c) TEM image of naked MSNs; d) TEM image of Dox-loaded pHLIPss-MSNs.

functionalized with amino groups via aminopropyltriethoxysilane (APTES). Following this, pHLIPss containing a free cysteine residue were immobilized on MSN surfaces by the heterobifunctional crosslinker sulfo-SMCC (Figure 1a). Such functionalization processes were monitored by Zeta potential. The surface Zeta potentials of MSN, amino-functionalized MSN, and peptide-functionalized MSN were −13 mV, 18 mV, and −17.9 mV, respectively. Further, Dox-loaded pHLIPss-MSNs were analyzed by small-angle X-ray diffraction (XRD), TEM, and N_2 adsorption–desorption isotherm. These results indicated that Dox-loaded pHLIPss-MSNs remained in their mesoporous state, showing that the functionalization and subsequent Dox-loaded process did not affect the mesoporous structure of MSN (Figure 1b, Figure S1b and Table S2).

To demonstrate whether pHLIPss could enhance targeting and translocation of MSNs at pH 6.5 compared to pH 7.4 as reported for pHLIP conjugated to other cargo,[11,13] for example, impermeable phalloidin, we tested the targeting and translocation of pHLIPss-MSNs in different cell lines at pH 6.5 and pH 7.4 by flow cytometry. As shown in Figure 2, pHLIPss-MSNs demonstrated greater targeting and translocation in MCF-7 cells and MCF-7/ADR at pH 6.5 than at pH 7.4 after 2 h incubation. However, this phenomenon was not observed in cells treated with MSNs modified with control

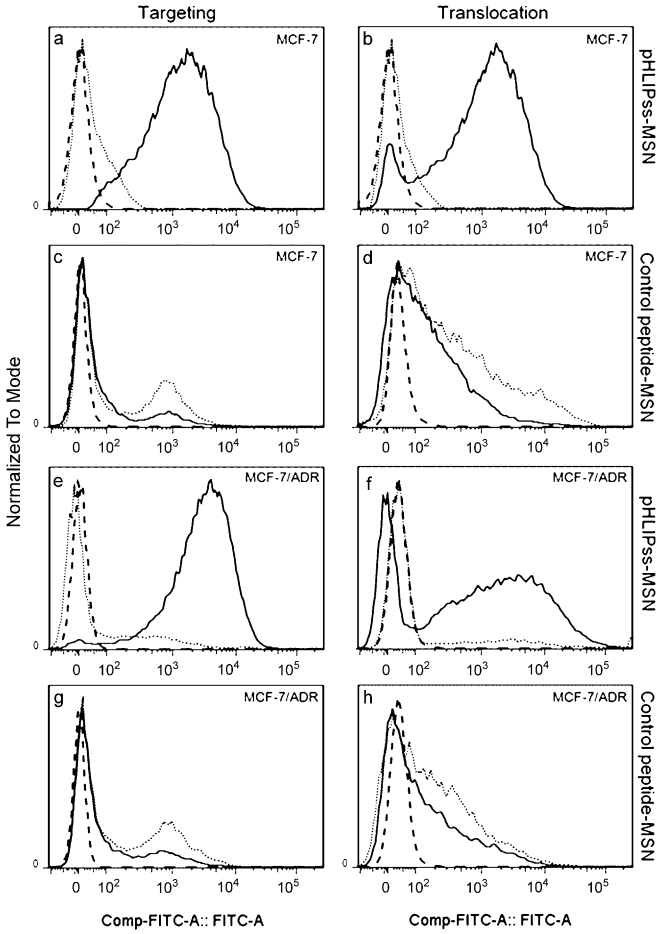

Figure 2. Flow cytometry analysis of the targeting (a, c, e, g) and translocation (b, d, f, h) of pHLIPss-MSNs (a, b, e, f) or control peptide-MSNs (c, d, g, h) in MCF-7 and MCF-7/ADR cell lines at pH 6.5 or pH 7.4. Dashed lines indicate auto-fluorescence of untreated cells. The fluorescence shift of cells treated with peptide-MSNs at pH 7.4 (dotted lines) and 6.5 (solid lines). To discriminate the subtle difference of translocation caused by control peptide-MSNs at different pH values, the excitation voltage in translocation analysis was adjusted to 200 V from the 150 V used in targeting analysis.

peptide. Enhanced targeting and translocation of nanocarrier caused by pHLIPss at pH 6.5 were also seen in A549 cells, U20S cells, H1299 cells, and HepG2 cells (Figure S3–S6). Moreover, the pHLIPss-MSN nanocarrier showed similar targeting and translocation in MCF-7 cells and MCF-7 treated with 0.25% trypsin for 5 min to partially destroy membrane protein (Figure S7). These results indicate that both targeting and translocation of the nanocarrier driven by low pH value were insensitive to cellular surface proteins and the heterogeneity among cancer cells, suggesting that the nanocarrier may be used in a broad spectrum of cancers for drug delivery. It was noted that pHLIPss-MSNs showed less targeting and translocation in MCF-7 cells and MCF-7/ADR cells than the control peptide-MSNs at pH 7.4, indicating that the system had little non-specific interaction at physiological pH value. The enhanced targeting of pHLIPss-MSNs in MCF-7 cells and MCF-7/ADR cells driven by low pH value was also confirmed by confocal laser scanning microscopy (Figure S8 and S9). In addition, the translocation of pHLIPss-MSNs at pH 6.5 could be seen within twenty minutes and did not depend on incubation time (Figure S10); however, the uptake of pHLIPss-MSNs at pH 7.4 showed time-dependent increase, suggesting that the cellular uptake of pHLIPss-MSNs at pH 6.5 and pH 7.4 may be mediated by different pathways.

It has been demonstrated that the translocation of cargo by pHLIP is triggered by the formation of a helix across the lipid bilayer as a result of the protonation of Asp residues induced by low pH values, rather than mediation by endocytosis or interactions with cell receptors.[11,14a] To test whether the translocation of our nanocarrier is also mediated by the same pathway, the reverse of translocation of MSNs modified with pHLIPss or pHLIPf containing no disulfide in MCF-7 cells was tested. As expected, the translocation of MSNs modified with pHLIPf in MCF-7 cells at pH 6.5 was easily reversed by washing with buffer at pH 7.4 (Figure 3a). However, the fluorescence shift caused by pHLIPss-MSNs was only partially reversed by washing with buffer at pH 7.4 (Figure 3b). These experiments demonstrate that the translocation mechanism of pHLIPss-MSNs at pH 6.5 is mainly mediated by pHLIPss which insert into the membrane at low pH value and then directly translocate MSNs into cell cytoplasm, rather than internalization or endocytosis.

We also compared the pH_e-targeting and the translocation ability of pHLIPss-MSNs and pHLIPss. It was observed that pHLIPss-MSNs caused a significantly greater fluorescence signal in cultured cells than individual pHLIPss under the same conditions (Figure S11). This enhancement may be caused by the high local concentration of pHLIPss on the surface of MSN (about 1.3 micromoles per g MSN). Moreover, the stabilities of pHLIPss-MSNs and pHLIPss in human serum were examined by testing their translocation ability in MCF-7 cells (Figure S12). With increasing incubation time, the translocation ability of pHLIPss-MSNs and pHLIPss decreased gradually. However, after 12 h incubation in human serum, pHLIPss-MSNs, rather than pHLIPss, retained its translocation ability. These results suggest that MSN may partially protect the peptide from hydrolysis in serum. Thus, the functional integration of pHLIPss and MSN makes pHLIPss-MSNs promising in the development of a pH_e-targeted nanocarrier for drug delivery.

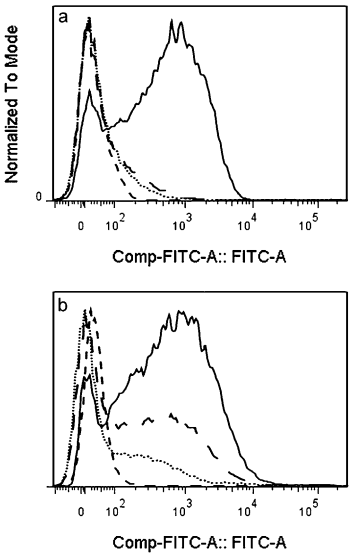

Figure 3. Flow cytometry analysis of the reverse of translocation of pHLIPf-MSNs (a) or pHLIPss-MSNs (b) in MCF-7 cells after 2 h incubation with washing buffer at pH 7.4. Dashed lines (lower trace) indicate auto-fluorescence untreated cells. The fluorescence shift of cells treated with peptide-MSNs at pH 7.4 followed by washing with PBS (7.4; dotted lines), at pH 6.5 followed by washing with PBS (pH 6.5; solid lines), and at pH 6.5 followed by washing with PBS (pH 7.4; long dashed lines, upper trace).

To investigate the drug release of pHLIPss-MSNs, 10 mg of Dox-loaded pHLIPss-MSNs were added to 1 mL of PBS with or without 30 mM dithiothreitol (DTT). The release of Dox from nanocarrier was assessed by measuring its fluorescence at 580 nm. As shown in Figure 4a, about 16% release occurred in the absence of DTT after 16 h. However, a significant release was found after 5 h in PBS with DTT owing to the cleavage of the disulfide bond by DTT (Figure 4a). The excellent pore-capping property of pHLIPss on MSN may be cooperatively caused by the following two factors: 1) the amount and length of pHLIPss peptide on MSNs covers the pore;[16] 2) electrostatic interaction between the negatively charged peptide and the positively charged amino-functionalized MSNs.[15] The release induced by cleavage of the disulfide bond was also observed in MCF-7 cells treated with Dox-loaded pHLIPss-MSNs for 24 h, where Dox was found to accumulate in the nucleus (Figure 4b). However, no accumulation of Dox in the nucleus was seen in MCF-7 cells treated with Dox-loaded pHLIPf-MSNs for 24 h (Figure 4b). These results indicate that the introduction of the disulfide bond in the nanocarrier makes drug release controllable.

To test the cytotoxicity of the Dox-loaded pHLIPss-MSNs nanocarrier with low pH-driven targeting and translocation, we assessed its cytotoxicity in two cell lines: drug-sensitive MCF-7 cells and drug-resistant MCF-7/ADR cells. After being incubated with Dox-loaded pHLIPss-MSNs or empty pHLIPss-MSNs for 3 h at pH 6.5 or pH 7.4, the cells were grown in normal cell medium for another 72 h. Following this

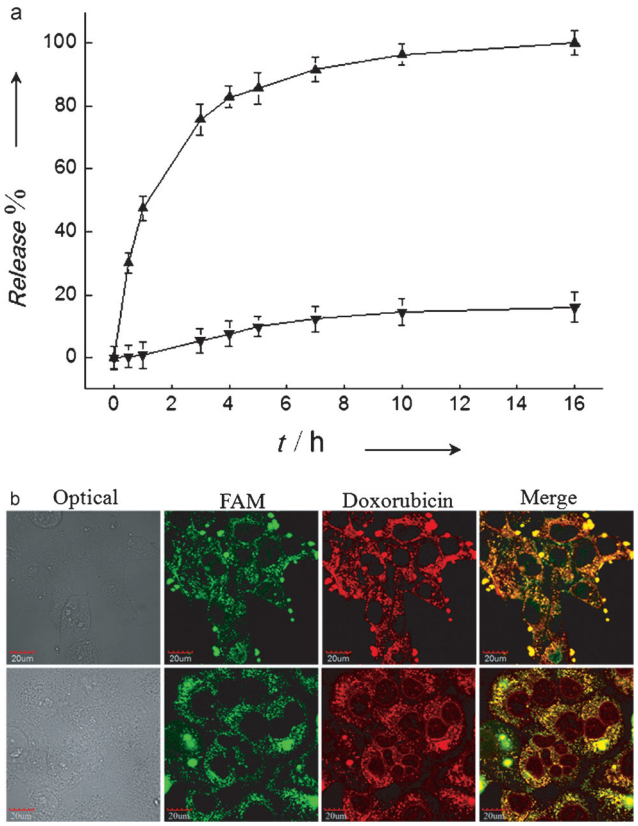

Figure 4. a) Release kinetics of doxorubicin from pHLIPss-MSNs in the presence (▲) and absence of dithiothreitol (▼) at pH 7.4. Error bars indicate the standard deviation of three separated experiments. b) Confocal fluorescence images of Dox distribution in MCF-7 cells treated with Dox-loaded pHLIPf-MSNs (upper) and Dox-loaded pHLIPss-MSNs (lower) at pH 6.5 for 24 h.

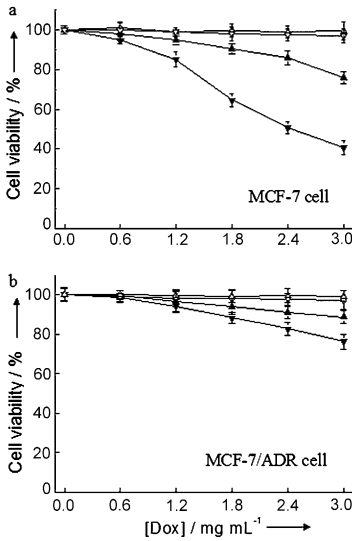

Figure 5. Viability of a) MCF-7 cells and b) MCF-7/ADR cells treated with Dox-loaded pHLIPss-MSNs at pH 6.5 (▼) and at pH 7.4 (▲), or empty pHLIPss-MSNs at pH 6.5 (▽) and pH 7.4 (△). Errors bars indicate the standard deviation of three separate experiments.

step, MTS assay was used to assess cell viability. The results summarized in Figure 5 show that Dox-loaded pHLIPss-MSNs provide significantly enhanced antiproliferation in MCF-7 cells and MCF-7/ADR cells at pH 6.5 relative to those at pH 7.4, and the growth inhibition on these cells is dosage-dependent. At an equivalent Dox concentration of 3 $\mu g\,mL^{-1}$, growth inhibition of Dox-load nanocarrier was 60 % at pH 6.5 and 25 % at pH 7.4 for MCF-7 cells, and about 25 % at pH 6.5 and 10 % at pH 7.4 for MCF-7/ADR cells. Compared with free Dox at pH 6.5, Dox-loaded pHLIPss-MSN showed better cytotoxicity (Figure S13). However, the empty pHLIPss-MSNs without Dox did not show cytotoxicity under the same conditions up to a concentration of 100 $\mu g\,mL^{-1}$.

In summary, as a proof-of-concept, we have demonstrated that it is possible to program mesoporous silica nanoparticles with a peptide to construct an efficient and controlled-release nanocarrier that actively targets and directly translocates into cells once exposed to tumor extracellular pH value, subsequently releasing its payload through cleavage of the disulfide bonds by reduced glutathione in the cytoplasm. This pH_e-targeted drug delivery system results in enhanced cytotoxicity for both drug-sensitive and drug-resistant tumor cells in vitro at pH 6.5 compared to at pH 7.4. Our Dox-loaded pHLIPss-MSNs nanocarrier has the following advantages: 1) pH_e-driven targeting and translocation, which can bypass biomarker-targeting molecules, thus avoiding sensitivity to heterogeneous expression of different cancer cells; 2) translocation which is not mediated by endocytosis or by interaction with a receptor; 3) release of payload only upon the cleavage of peptide from MSN caused by cytoplasmic glutathione; 4) simple construction from custom-made materials and commercially available peptide. Although pHLIPss-MSNs retain their translocation response to low pH value after 12 h incubation in serum, we are aware that the stability of pHLIPss-MSNs in serum needs further improvement. However, we believe that the design of pH_e-targeted pHLIPss-MSNs nanocarrier, in which proper chemical modification or D-amino acids is used to enhance the stability of pHLIPss in serum, is promising as a tumor-targeted delivery platform.

Received: March 27, 2013
Published online: June 11, 2013

Keywords: drug delivery · mesoporous silica nanoparticle · nanocarriers · pHLIP · targeted release

[1] D. Peer, J. M. Karp, S. Hong, O. C. Farokhzad, R. Margalit, R. Langer, *Nat. Nanotechnol.* **2007**, *2*, 751 – 760.
[2] H. Maeda, H. Nakamura, J. Fang, *Adv. Drug Delivery Rev.* **2013**, *65*, 71 – 79.
[3] R. Duncan, *Nat. Rev. Cancer* **2006**, *6*, 688 – 701.
[4] R. D. Hofheinz, S. U. Gnad-Vogt, U. Beyer, A. Hochhaus, *Anti-Cancer Drugs* **2005**, *16*, 691 – 707.
[5] C. H. Lee, S. H. Cheng, I. P. Huang, J. S. Souris, C. S. Yang, C. Y. Mou, L. W. Lo, *Angew. Chem.* **2010**, *122*, 8390 – 8395; *Angew. Chem. Int. Ed.* **2010**, *49*, 8214 – 8219.
[6] a) H. Maeda, G. Y. Bharate, J. Daruwalla, *Eur. J. Pharm. Biopharm.* **2009**, *71*, 409 – 419; b) T. M. Allen, P. R. Cullis, *Science* **2004**, *303*, 1818 – 1822.

[7] a) L. Brannon-Peppas, J. O. Blanchette, *Adv. Drug Delivery Rev.* **2004**, *56*, 1649 – 1659; b) Z. L. Cheng, A. A. Zaki, J. Z. Hui, V. R. Muzykantov, A. Tsourkas, *Science* **2012**, *338*, 903 – 910; c) J. V. Georgieva, R. P. Brinjhuis, K. Stojanov, C. A. Weijers, H. Zuilhof, F. P. Rutjes, D. Hoekstra, J. C. Van Hest, I. S. Zuhorn, *Angew. Chem.* **2012**, *124*, 8464 – 8467; *Angew. Chem. Int. Ed.* **2012**, *51*, 8339 – 8342; d) T. Chen, M. I. Shukoor, Y. Chen, Q. Yuan, Z. Zhu, Z. Zhao, B. Gulbakan, W. Tan, *Nanoscale* **2011**, *3*, 546 – 556; e) O. C. Farokhzad, J. M. Karp, R. Langer, *Expert Opin. Drug Delivery* **2006**, *3*, 311 – 324.

[8] Y. H. Bae, K. Park, *J. Controlled Release* **2011**, *153*, 198 – 205.

[9] a) C. W. Li, D. G. Heidt, P. Dalerba, C. F. Burant, L. J. Zhang, V. Adsav, M. Wicha, M. F. Clarke, D. M. Simeone, *Cancer Res.* **2007**, *67*, 1030 – 1037; b) E. J. Fox, J. J. Salk, L. A. Loeb, *Cancer Res.* **2009**, *69*, 4948 – 4950.

[10] a) P. Vaupel, F. Kallinowski, P. Okunieff, *Cancer Res.* **1989**, *49*, 6449 – 6465; b) L. E. Gerweck, K. Seetharaman, *Cancer Res.* **1996**, *56*, 1194 – 1198; c) W. Gao, J. M. Chan, O. C. Farokhzad, *Mol. Pharm.* **2010**, *7*, 1913 – 1920; d) E. S. Lee, Z. G. Gao, Y. H. Bae, *J. Controlled Release* **2008**, *132*, 164 – 170.

[11] M. An, D. Wijesinghe, O. A. Andreev, Y. K. Reshetnyak, D. M. Engelman, *Proc. Natl. Acad. Sci. USA* **2010**, *107*, 20246 – 20250.

[12] a) X. L. Wu, J. H. Kim, H. Koo, S. M. Bae, H. Shin, M. S. Kim, B. H. Lee, R. W. Park, I. S. Kim, K. Choi, I. C. Kwon, K. Kim, D. S. Lee, *Bioconjugate Chem.* **2010**, *21*, 208 – 213; b) E. S. Lee, K. Na, Y. H. Bae, *Nano Lett.* **2005**, *5*, 325 – 329; c) J. Z. Du, T. M. Sun, W. J. Song, J. Wu, J. Wang, *Angew. Chem.* **2010**, *122*, 3703 – 3708; *Angew. Chem. Int. Ed.* **2010**, *49*, 3621 – 3626; d) J. Z. Du, X. J. Du, C. Q. Mao, J. Wang, *J. Am. Chem. Soc.* **2011**, *133*, 17560 – 17563; e) E. S. Lee, Z. Gao, D. Kim, K. Park, I. C. Kwon, Y. H. Bae, *J. Controlled Release* **2008**, *129*, 228 – 236; f) V. A. Sethuraman, Y. H. Bae, *J. Controlled Release* **2007**, *118*, 216 – 224; g) E. Jin, B. Zhang, X. Sun, Z. Zhou, X. Ma, Q, Sun, J. Tang, Y. Shen, E. Van Kirk, W. J. Murdoch, M. Radosz, *J. Am. Chem. Soc.* **2013**, *135*, 933 – 940.

[13] a) Y. K. Reshetnyak, O. A. Andreev, U. Lehnert, D. M. Engelman, *Proc. Natl. Acad. Sci. USA* **2006**, *103*, 6460 – 6465; b) Y. K. Reshetnyak, O. A. Andreev, M. Segala, V. S. Markin, D. M. Engelman, *Proc. Natl. Acad. Sci. USA* **2008**, *105*, 15340 – 15345; c) O. A. Andreev, A. G. Karabadzhak, D. Weerakkody, G. O. Andreev, D. M. Engelman, Y. K. Reshetnyak, *Proc. Natl. Acad. Sci. USA* **2010**, *107*, 4081 – 4086; d) O. A. Andreev, A. D. Dupuy, M. Segala, S. Sandugu, D. A. Serra, C. O. Chichester, D. M. Engelman, Y. K. Reshetnyak, *Proc. Natl. Acad. Sci. USA* **2007**, *104*, 7893 – 7898; e) A. Davies, D. J. Lewis, S. P. Watson, S. G. Thomas, Z. Pikramenou, *Proc. Natl. Acad. Sci. USA* **2012**, *109*, 1862 – 1867; f) L. Yao, J. Danniels, A. Moshnikova, S. Kuznetsov, A. Ahmed, D. M. Engelman, Y. K. Reshetnyak, O. A. Andreev, *Proc. Natl. Acad. Sci. USA* **2013**, *110*, 465 – 470.

[14] a) M. Vallet-Regí, F. Balas, D. Arcos, *Angew. Chem.* **2007**, *119*, 7692 – 7703; *Angew. Chem. Int. Ed.* **2007**, *46*, 7548 – 7558; b) C. Coll, A. Bernardos, R. Martínez-Máñez, F. Sancenón, *Acc. Chem. Res.* **2013**, *46*, 339 – 349; c) C. E. Ashley, E. C. Carnes, G. K. Phillips, D. Padilla, P. N. Durfee, P. A. Brown, T. N. Hanna, J. Liu, B. Phillips, M. B. Carter, N. J. Carroll, X. Jiang, D. R. Dunphy, C. L. Willman, D. N. Petsev, D. G. Evans, A. N. Parikh, B. Chackerian, W. Wharton, D. S. Peabody, C. J. Brinker, *Nat. Mater.* **2011**, *10*, 389 – 397.

[15] a) E. Climent, R. Martínez-Máñez, F. Sancenón, M. D. Marcos, J. Soto, A. Maquieira, P. Amorós, *Angew. Chem.* **2010**, *122*, 7439 – 7441; *Angew. Chem. Int. Ed.* **2010**, *49*, 7281 – 7283; b) Q. Yuan, Y. F. Zhang, T. Chen, D. Q. Lu, Z. L. Zhao, X. B. Zhang, Z. Li, C. H. Yan, W. H. Tan, *ACS Nano* **2012**, *6*, 6337 – 6344.

[16] C. Coll, L. Mondragón, R. Martínez-Máñez, F. Sancenón, M. D. Marcos, J. Soto, P. Amorós, E. Pérez-Payá, *Angew. Chem.* **2011**, *123*, 2186 – 2188; *Angew. Chem. Int. Ed.* **2011**, *50*, 2138 – 2140.

